

See discussions, stats, and author profiles for this publication at: <https://www.researchgate.net/publication/8008659>

Photochromic Control of Photoinduced Electron Transfer. Molecular Double-Throw Switch

ARTICLE *in* JOURNAL OF THE AMERICAN CHEMICAL SOCIETY · APRIL 2005

Impact Factor: 12.11 · DOI: 10.1021/ja044128i · Source: PubMed

CITATIONS

66

READS

29

6 AUTHORS, INCLUDING:



[Joakim Andreasson](#)

Chalmers University of Technology

58 PUBLICATIONS 2,364 CITATIONS

[SEE PROFILE](#)



[Gerdenis Kodis](#)

Arizona State University

75 PUBLICATIONS 2,399 CITATIONS

[SEE PROFILE](#)



[Thomas A Moore](#)

Arizona State University

331 PUBLICATIONS 16,788 CITATIONS

[SEE PROFILE](#)

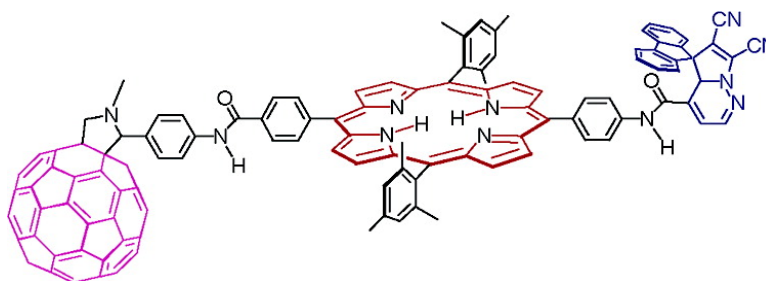
Article

Photochromic Control of Photoinduced Electron Transfer. Molecular Double-Throw Switch

Stephen D. Straight, Joakim Andrasson, Gerdenis Kodis, Ana L. Moore, Thomas A. Moore, and Devens Gust

J. Am. Chem. Soc., **2005**, 127 (8), 2717-2724 • DOI: 10.1021/ja044128i

Downloaded from <http://pubs.acs.org> on December 17, 2008



More About This Article

Additional resources and features associated with this article are available within the HTML version:

- Supporting Information
- Links to the 22 articles that cite this article, as of the time of this article download
- Access to high resolution figures
- Links to articles and content related to this article
- Copyright permission to reproduce figures and/or text from this article

[View the Full Text HTML](#)



ACS Publications
High quality. High impact.

Photochromic Control of Photoinduced Electron Transfer. Molecular Double-Throw Switch

Stephen D. Straight, Joakim Andréasson, Gerdenis Kodis, Ana L. Moore,*
Thomas A. Moore,* and Devens Gust*

*Contribution from the Department of Chemistry and Biochemistry, Center for the Study of Early
Events in Photosynthesis, Arizona State University, Tempe, Arizona 85287*

Received September 27, 2004; E-mail: gust@asu.edu

Abstract: A molecular double-throw switch that employs a photochromic moiety to direct photoinduced electron transfer from an excited state donor down either of two pathways has been prepared. The molecular triad consists of a free base porphyrin (P) linked to both a C₆₀ electron acceptor and a dihydroindolizine (DHI) photochrome. Excitation of the porphyrin moiety of DHI–P–C₆₀ results in photoinduced electron transfer with a time constant of 2.3 ns to give the DHI–P⁺–C₆₀^{•–} charge-separated state with a quantum yield of 82%. UV (366 nm) light photoisomerizes the DHI moiety to the betaine (BT) form, which has a higher reduction potential than DHI. Excitation of the porphyrin of BT–P–C₆₀ is followed by photoinduced electron transfer with a time constant of 56 ps to produce BT^{•–}–P⁺–C₆₀ in 99% yield. Isomerization of BT–P–C₆₀ back to DHI–P–C₆₀ may be achieved with visible light, or thermally. Thus, photoinduced charge separation originating from the porphyrin is reversibly directed down either of two different pathways by photoisomerization of the dihydroindolizine. The switch may be cycled many times.

Introduction

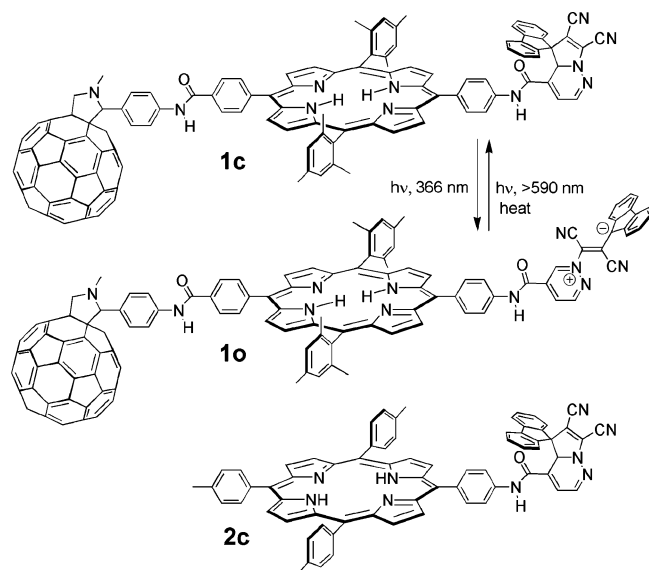
Photoinduced electron transfer is the basis of photosynthetic conversion of light energy into useful electrochemical potential and is important in a variety of technological applications. The promise of using such a process in molecular-scale optoelectronics has prompted researchers to develop ways to control photoinduced electron transfer using light or other inputs. Photochromic molecules, which can be isomerized between two thermally stable molecular structures using light, are good candidates for light-activated control units in molecule-based devices of various types.^{1–6} Recently, we have demonstrated on and off switching of photoinduced electron transfer in molecular dyads and triads by using photochromes to reversibly quench excited singlet states via energy transfer,^{7,8} reversibly alter reduction potentials of electron acceptors,⁹ and reversibly change oxidation potentials of electron donor moieties.¹⁰ The

electrical analogue of these molecular switches is the simple single-throw switch, in which current is passed in the on position, and the circuit is interrupted in the off position. In the present work, we have investigated a method for using light excitation to direct electron transfer from an excited singlet state of a donor down either of two different pathways. Such molecular switches are analogues of the electrical double-throw switch, which connects an input to either of two different circuits. In other approaches to bidirectional photoinduced electron transfer, Wasielewski and co-workers have reported a system in which the initial photoinduced electron-transfer always occurs along the same pathway, but a second femtosecond laser pulse initiates a charge-shift reaction that moves the electron to another pathway.¹¹ The direction of a photocurrent has recently been controlled by selective excitation of either of two chromophores in separate molecules tethered to a gold surface by polypeptides.¹² The approach used here employs a photochromic dihydroindolizine (DHI) covalently linked to a porphyrin (P), which also bears a fullerene moiety (C₆₀) to form triad **1** (Chart 1). Since our first report of photoinduced electron transfer in a covalently linked porphyrin–fullerene dyad,¹³ many researchers have demonstrated photoinduced electron transfer from the first excited singlet state of a porphyrin to an attached fullerene. Such transfer is characterized by rapid charge separation and relatively slow charge recombination. Also, we have recently reported the preparation and study of DHI–P dyad molecular switch **2**.⁹ In

- (1) Katz, E.; Willner, B.; Willner, I. *Biosens. Bioelectron.* **1997**, *12*, 703–719.
- (2) Mitchell, R. H.; Ward, T. R.; Chen, Y.; Wang, Y.; Weerawarna, S. A.; Dibble, P. W.; Marsella, M. J.; Almutairi, A.; Wang, Z. Q. *J. Am. Chem. Soc.* **2003**, *125*, 2974–2988.
- (3) Willner, I.; Doron, A.; Katz, E. *J. Phys. Org. Chem.* **1998**, *11*, 546–560.
- (4) Fernandez-Acebes, A.; Lehn, J.-M. *Chemistry–Eur. J.* **1999**, *5*, 3285–3292.
- (5) Norsten, T. B.; Branda, N. R. *J. Am. Chem. Soc.* **2001**, *123*, 1784–1785.
- (6) Walz, J.; Ulrich, K.; Port, H.; Wolf, H. C.; Wöhrner, J.; Effenberger, F. *Chem. Phys. Lett.* **1993**, *213*, 321–324.
- (7) Liddell, P. A.; Kodis, G.; Moore, A. L.; Moore, T. A.; Gust, D. *J. Am. Chem. Soc.* **2002**, *124*, 7668–7669.
- (8) Bahr, J. L.; Kodis, G.; de la Garza, L.; Lin, S.; Moore, A. L.; Moore, T. A.; Gust, D. *J. Am. Chem. Soc.* **2001**, *123*, 7124–7133.
- (9) Terazono, Y.; Kodis, G.; Andréasson, J.; Jeong, G.; Brune, A.; Hartmann, T.; Dürr, H.; Moore, A. L.; Moore, T. A.; Gust, D. *J. Phys. Chem. B* **2004**, *108*, 1812–1814.
- (10) Liddell, P. A.; Kodis, G.; Andréasson, J.; de la Garza, L.; Bandyopadhyay, S.; Mitchell, R. H.; Moore, T. A.; Moore, A. L.; Gust, D. *J. Am. Chem. Soc.* **2004**, *126*, 4803–4811.

- (11) Lukas, A. S.; Miller, S. E.; Wasielewski, M. R. *J. Phys. Chem. B* **2000**, *104*, 931–940.
- (12) Yasutomi, S.; Morita, T.; Imanishi, Y.; Kimura, S. *Science* **2004**, *304*, 1944–1947.
- (13) Liddell, P. A.; Sumida, J. P.; Macpherson, A. N.; Noss, L.; Seely, G. R.; Clark, K. N.; Moore, A. L.; Moore, T. A.; Gust, D. *Photochem. Photobiol.* **1994**, *60*, 537–541.

Chart 1

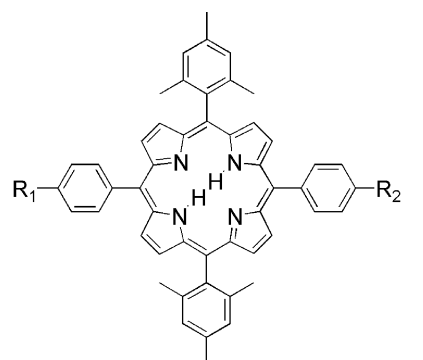


the closed, spirocyclic dihydroindolizine form **2c** (Chart 1), excitation of the porphyrin moiety in the 2-methyltetrahydrofuran solution is followed by normal deactivation of the excited singlet state via the usual photophysical processes of internal conversion, intersystem crossing, and fluorescence ($\tau = 11.5$ ns). The porphyrin excited state is not perturbed by the attached dihydroindolizine. Irradiation of DHI-P with UV (366 nm) light photoisomerizes the DHI to the open, betaine form BT (**2o**, analogous to **1o**), which is much more easily reduced than the DHI form. Excitation of the porphyrin moiety of BT-P is followed by rapid ($\tau = 50$ ps) photoinduced electron transfer to the BT, yielding a short-lived $\text{BT}^{\bullet-}-\text{P}^{\bullet+}$ charge-separated state. Therefore, we reasoned that if a fullerene was covalently linked to the porphyrin of a molecule like **2** in such a way that photoinduced electron transfer from the porphyrin first excited singlet state to the C_{60} occurred much more slowly than electron transfer to BT, a photochromically controlled molecular double-throw switch could be prepared. A recent report¹⁴ suggested that the linkage shown in **1** should provide a suitable transfer rate, and this has now been verified by study of model P- C_{60} dyad **9**. Indeed, the double-throw switch does perform as envisioned, as described next.

Results

Synthesis. Synthesis began with the preparation of previously known porphyrin **4** from **3** (Chart 2).¹⁵ The carboxylic acid group of **4** was protected as the *t*-butyl ester (**5**), and the amino group was coupled to pyridazine 4-carboxylate using 1-[3-(dimethylamino)propyl]-3-ethylcarbodiimide and 4-(dimethylamino)pyridine to obtain **6**. This precursor was allowed to react with spiro[fluorene-9,3'-[3H]pyrazole]-4',5'-dicarbonitrile under UV irradiation to yield DHI-P dyad **8** (Chart 3) and an isomer resulting from reaction at the second pyridazine nitrogen, which were separated chromatographically. Treatment of **8** with triethylsilane and trifluoroacetic acid removed the protecting group from the carboxylic acid. Meanwhile, fullerene precursor

Chart 2



3: $\text{R}_1 = \text{R}_2 = \text{COOCH}_3$

4: $\text{R}_1 = \text{COOH}$, $\text{R}_2 = \text{NH}_2$

5: $\text{R}_1 = \text{COOC}(\text{CH}_3)_3$, $\text{R}_2 = \text{NH}_2$

6: $\text{R}_1 = \text{COOC}(\text{CH}_3)_3$, $\text{R}_2 =$

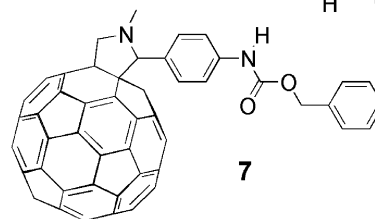
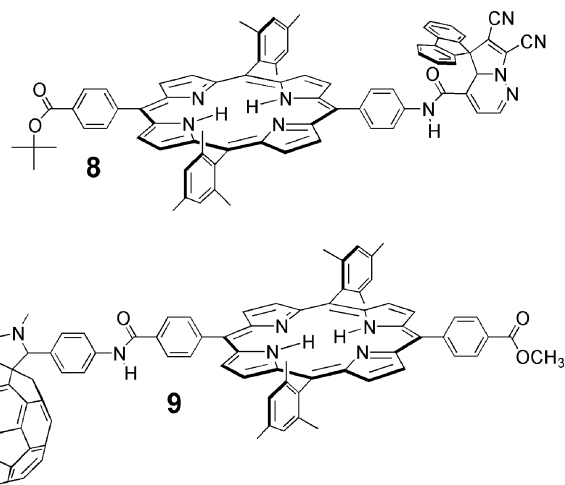


Chart 3



7 was deprotected by treatment with boron tribromide. The fullerene amine and porphyrin acid were coupled using 1,3-dicyclohexylcarbodiimide to give triad **1**. The model porphyrin-fullerene dyad **9** was prepared using similar methods. The details and characterization data are given in the Experimental Procedures.

Photochemistry. We will first describe the photochemistry of model P- C_{60} dyad **9** and model DHI-P **2** and then consider the results for triad **1**.

P- C_{60} Dyad 9. The absorption spectrum of **9** in the 2-methyltetrahydrofuran solution is shown in Figure 1. Porphyrin absorption maxima are observed at 418 (Soret), 482, 514, 547, 593, and 648 nm. The fullerene absorbs very weakly throughout the visible, with its longest wavelength absorption

(14) Tkachenko, N. V.; Vehmanen, V.; Nikkanen, J.; Yamada, H.; Imahori, H.; Fukuzumi, S.; Lemmetyinen, H. *Chem. Phys. Lett.* **2002**, *366*, 245–252.
 (15) Liddell, P. A.; Kodis, G.; de la Garza, L.; Bahr, J. L.; Moore, A. L.; Moore, T. A.; Gust, D. *Helv. Chim. Acta* **2001**, *84*, 2765–2783.

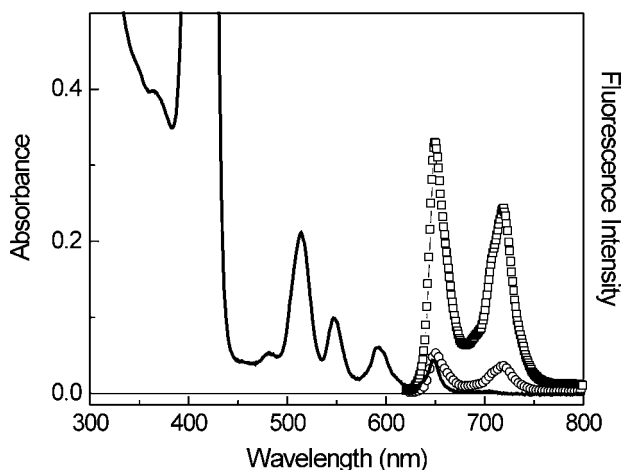


Figure 1. Absorption spectrum of P-C₆₀ dyad **9** (—) in 2-methyltetrahydrofuran and fluorescence spectra of **9** (○) and model porphyrin **3** (□) with the same absorbance at the 590 nm excitation wavelength.

band at 704 nm. These absorption bands are virtually unchanged from those of model porphyrins such as **3** and model fullerenes such as **7**.

The fluorescence spectra of dyad **9** and model porphyrin **3** in 2-methyltetrahydrofuran, both solutions having the same absorbance at the excitation wavelength of 590 nm, are also shown in Figure 1. The emission spectra of **9** and **3** are of virtually identical shape and are typical of free base porphyrins of this type, with maxima at 650 and 720 nm. However, the emission from the dyad is quenched relative to **3** by a factor of about 6. This quenching is ascribed to photoinduced electron transfer from the porphyrin to the fullerene to generate a P^{•+}–C₆₀^{•–} charge-separated state.

To more fully investigate the formation of the charge-separated state, time-resolved fluorescence experiments were undertaken in 2-methyltetrahydrofuran. A solution (~1 × 10^{–5} M) of **3** was excited at 590 nm, and emission was measured at 720 nm. The data were fitted by a single-exponential decay with a lifetime of 10.1 ns (χ² = 1.12). The data for dyad **9** required two exponentials, with time constants of 2.0 ns (99.4%) and 11.0 ns (0.6%) (χ² = 1.09). The low-amplitude component with the 11.0 ns lifetime is ascribed to an impurity. Thus, the time-resolved data confirm the substantial quenching of the porphyrin first excited singlet state by the attached fullerene.

The charge separation process was also examined using transient absorption spectroscopy. Figure 2 shows the results of excitation of the porphyrin moiety of **9** with ~100 fs laser pulses at 650 nm. The inset in Figure 2a shows the transient absorption spectrum in the 1000 nm region taken 3.0 ns after the laser pulse. The transient has a maximum at about 1010 nm that is characteristic of the fullerene radical anion of the P^{•+}–C₆₀^{•–} state. The kinetics at this wavelength, also shown in Figure 2a, was fitted with two exponential components following the laser pulse: a 2.0 ns rising component and a 4 ns decay. The 2.0 ns component is ascribed to formation of P^{•+}–C₆₀^{•–} and the 4 ns component to decay of this species. This interpretation is consistent with the decay-associated spectra obtained in the visible region and shown in Figure 2b. The spectrum with the 2.0 ns time constant indicates decay of the porphyrin first excited singlet state and concurrent formation of the P^{•+}–C₆₀^{•–} charge-separated state. The 4 ns component,

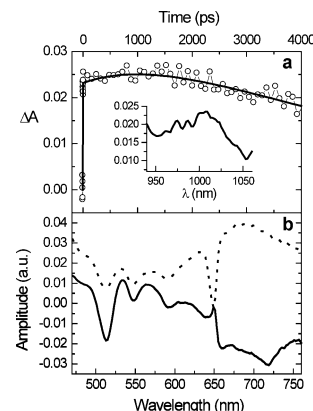


Figure 2. Transient absorption data for P-C₆₀ dyad **9** in 2-methyltetrahydrofuran following excitation at 650 nm. (a) Rise and decay of the transient absorption at 1010 nm of the fullerene radical anion of P^{•+}–C₆₀^{•–} (○) and fit to two exponential components with lifetimes of 2.0 and 4 ns (—). The prompt rise occurs with the excitation pulse and is ascribed to the formation of excited singlet states. The inset shows the spectrum taken 3.0 ns after excitation. (b) Decay-associated spectra for the same solution and measured in the visible region. The two components have lifetimes of 2.0 ns (—) and 4 ns (---). The spectral shapes near 650 nm are somewhat distorted due to the excitation pulse.

with characteristic absorption of the porphyrin radical cation around 700 nm, corresponds to the decay of P^{•+}–C₆₀^{•–}. (The short time window available in the experiment limits the precision of this time constant.)

DHI–P Dyad 2. The properties of model dyad **2** have been reported previously⁹ and are summarized here for use in later discussions. The absorption spectrum of DHI–P (**2c**) in 2-methyltetrahydrofuran in the visible region is characteristic of an unperturbed tetra-arylporphyrin with maxima at 419, 483, 515, 550, 593, and 650 nm. The emission from DHI–P is also unperturbed, with maxima at 655 and 721 nm and an excited-state lifetime of 11.5 ns. Thus, the DHI moiety has no significant effect upon the porphyrin excited singlet state.

When **2** is irradiated at 366 nm, DHI–P dyad **2c** is photoisomerized to the BT–P dyad (designated **2o**). The absorption spectrum of **2o** shows the broad betaine absorption underlying the porphyrin Q-bands. Porphyrin emission is observed, but it is very strongly quenched relative to **2c**. Transient absorption experiments showed that the quenching was due to photoinduced electron transfer from the porphyrin first excited singlet state to the betaine to yield a short-lived BT^{•–}–P^{•+} charge-separated state. The rate constant for photoinduced electron transfer is 2.0 × 10¹⁰ s^{–1} (τ = 50 ps, Φ = 1.0), and the rate constant for recombination is 3.4 × 10¹¹ s^{–1} (τ = 2.9 ps). The BT–P isomer **2o** may be isomerized back to the DHI form **2c** by irradiation at wavelengths ≥ 590 nm (Φ ~ 0.02),⁹ or thermally.

DHI–P–C₆₀ Triad 1. With the results for **2** and **9** as background, we turn our attention to DHI–P–C₆₀ triad **1**. Figure 3 shows the absorption spectra of **1** in 2-methyltetrahydrofuran. The DHI–P–C₆₀ form of the triad (**1c**), wherein the dihydroindolizine moiety is in the spirocyclic form, resembles the spectrum of model porphyrin **3** in the visible region, with bands at 419 (Soret), 483, 515, 550, 594, and 649 nm. As is the case for dyad **9**, the fullerene moiety absorbs throughout the visible, with its long wavelength maximum at 703 nm. Thus, the DHI and fullerene moieties do not perturb the shape of the porphyrin spectrum. After irradiation with UV light at 366 nm, the

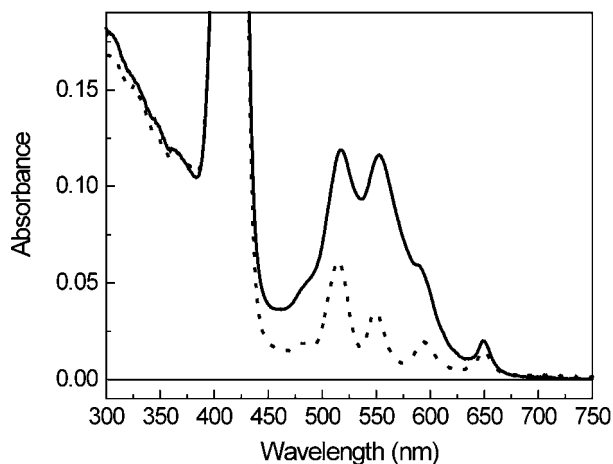


Figure 3. Absorption spectra of a sample of **1** in the DHI-P-C₆₀ closed form **1c** (---) and after conversion to a photostationary state consisting mainly of the BT-P-C₆₀ open form **1o** (—). The solvent was 2-methyltetrahydrofuran.

spectrum changes as shown in Figure 3. This is due to photoisomerization of the dihydroindolizine to yield the triad in the betaine form **1o**. The BT-P-C₆₀ triad has absorption maxima at 419, 485, 517, 552, 589, and 649 nm, plus the fullerene absorption mentioned previously. The change in appearance is due to the grow-in of the broad betaine absorption in the 550 nm region.⁹ The usual porphyrin absorption is superimposed upon this band. Thus, photoisomerization of the dihydroindolizine still occurs when it is linked to the porphyrin–fullerene dyad. This is vital to the proposed function of the switch molecule. The 366 nm irradiation creates a photostationary state; in deuteriochloroform, the ratio of the DHI form to the BT form in the model dihydroindolizine spiro[9H-fluorene-9,5'(4'aH)-pyrrolo[1,2-b]pyridazine]-6',7'-dicarbonitrile is 15:85, as determined by ¹H NMR experiments on ~0.02 M solutions. No line broadening or other effects suggestive of aggregation were noted in the NMR spectra. The molecule may be returned virtually entirely to the DHI form by irradiation with visible light ≥ 590 nm, or thermally.

The kinetics of the photoisomerization of **1** was investigated. When DHI-P-C₆₀ triad **1c** is irradiated at 366 nm with a light intensity of 1.5 mW/cm², the photostationary state consisting mainly of **1o** is reached with a time constant of 17 s. For the closing of BT-P-C₆₀ triad **1o**, isomerization under visible irradiation (≥ 590 nm, ~ 33 mW/cm²) occurs with a lifetime of 2400 s at 29 °C. At this temperature, the time constant for thermal closing of BT-P-C₆₀ is 4000 s. Thus, at ambient temperatures and with this light intensity, about 40% of the closing of the BT is photochemical, and 60% is thermally driven.

The porphyrin fluorescence of DHI-P-C₆₀ is comparable in intensity to that from model porphyrin–fullerene dyad **9**, but when the molecule is switched to the BT-P-C₆₀ form **1o**, the fluorescence is very strongly quenched. Time-resolved fluorescence measurements in 2-methyltetrahydrofuran yielded data for **1c** that were fitted ($\chi^2 = 1.08$) with two exponential components with time constants of 1.9 ns (86%) and 8.3 ns (14%). The 1.9 ns component is ascribed to the triad and the 8.3 ns component to a porphyrin impurity or decomposition product. After the molecule was opened to the BT-P-C₆₀ form **1o**, fitting the data ($\chi^2 = 1.17$) required components of 60 ps (76%), 1.7 ns (18%), and 9.4 ns (8%). The 60 ps

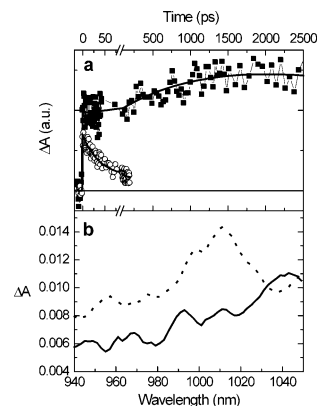


Figure 4. (a) Transient absorption results at 1000 nm for triad **1** following excitation of a 2-methyltetrahydrofuran solution at 650 nm with ~ 100 fs laser pulses. Data are for closed, DHI-P-C₆₀ triad **1c** (■) and open, BT-P-C₆₀ triad **1o** (○). During the experiments on **1o**, the sample was continuously irradiated at 366 nm to prevent any net photoisomerization to the closed form. The solid lines represent kinetic fits to the data. Please note the break in the time axis. (b) Transient absorption spectra taken 1.0 ns after excitation for the closed, DHI-P-C₆₀ triad (---) and 25 ps after excitation for the open, BT-P-C₆₀ triad (—).

component is due to BT-P-C₆₀, the 1.7 ns component to residual DHI-P-C₆₀ in the photostationary state, and the 9.4 ns component to porphyrin impurity.

Subpicosecond transient absorption measurements were used to further characterize the photochemistry of the triad in its two forms. Representative results are shown in Figure 4. The data for the closed DHI-P-C₆₀ triad **1c** in Figure 4b show that at 1.0 ns after the excitation pulse, there is clear evidence for an absorption maximum corresponding to the fullerene radical anion at ~ 1010 nm. This ion results from the DHI-P⁺-C₆₀^{•-} charge-separated state, as with model dyad **9**. The kinetic trace at 1000 nm (Figure 4a) shows the formation of DHI-P⁺-C₆₀^{•-} with a time constant of 2.0 ns and its decay with a lifetime of ~ 4 ns (the short time window available in this experiment limits the accuracy of this lifetime). In contrast, the results for BT-P-C₆₀ triad **1o** show no detectable fullerene radical anion absorption in the 1000 nm region (Figure 4b). The kinetic trace in Figure 4a shows only a decay of the porphyrin first excited singlet state absorption at 1000 nm on this time scale, with a time constant of 55 ps.

To obtain a better measurement of the decay of DHI-P⁺-C₆₀^{•-} in **1c**, transient absorbance experiments on the nanosecond time scale were performed. Figure 5 shows the kinetics at 1000 nm following excitation at 650 nm with 4.8 ns laser pulses. The formation of DHI-P⁺-C₆₀^{•-} is convoluted into the excitation pulse on this time scale, but the decay is seen to be biexponential, with a 4.7 ns decay constant and a component that does not decay on the time scale shown. The short component is ascribed to decay of DHI-P⁺-C₆₀^{•-} and the long component to the porphyrin and fullerene triplet excited states. The triplet states form via normal intersystem crossing in the porphyrin and possibly in part by recombination of DHI-P⁺-C₆₀^{•-}.

Figure 6 shows the effect of cycling the triad through a series of UV–vis cycles. The set of high (~ 0.015) absorbance values signifies the detection of the fullerene radical anion of DHI-P⁺-C₆₀^{•-} when the molecule is in the closed form **1c**. The set of low absorbance values was measured after the molecule was photoisomerized to the BT-P-C₆₀ state **1o**. To

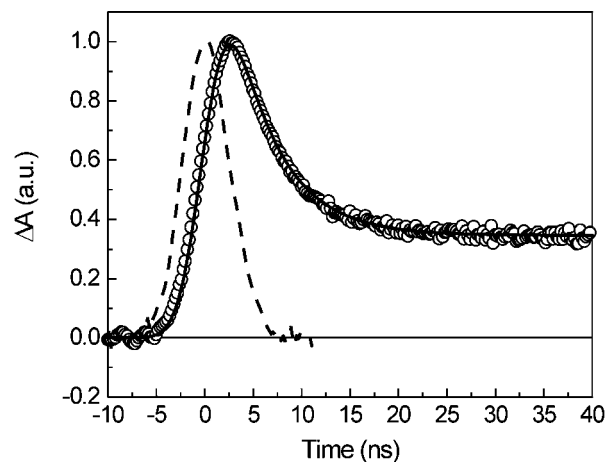


Figure 5. Transient absorption data (○) at 1000 nm obtained following excitation of a $\sim 1 \times 10^{-4}$ M solution of DHI-P-C₆₀ triad **1c** in 2-methyltetrahydrofuran by a 4.8 ns laser pulse at 650 nm. The solid line is a 2-exponential fit with a component that decays with a time constant of 4.7 ns and a nondecaying component. The dotted line is the spectrometer response function, showing that the formation of the transient absorbance is convoluted with the laser pulse.

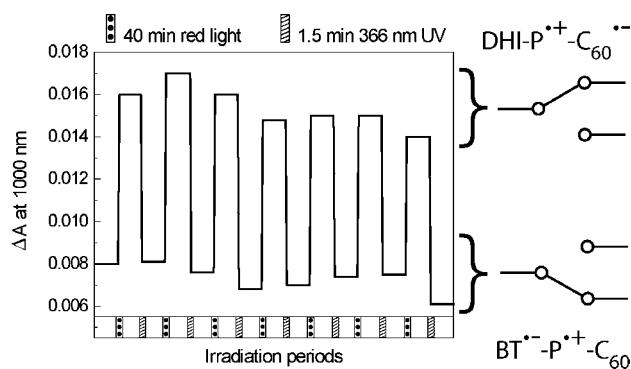


Figure 6. Photochemical cycling of the molecular double-throw switch **1**. The data are the amplitudes of the transient absorption at 1000 nm following laser excitation at 650 nm. High absorbance indicates the presence of the fullerene radical anion in DHI-P⁺-C₆₀^{•-}. Low absorbance indicates the absence of a fullerene radical anion in BT^{•-}-P⁺-C₆₀. At the beginning of the experiment (left side of the figure), the molecule is in the betaine form **1o**. Red (≥ 590 nm) light excitation converts the molecule to the DHI form **1c**. Excitation at 366 nm converts **1c** back to **1o**. The position of the double-throw switch is shown schematically at the right.

obtain these data, the transient absorbance of the molecule in the BT-P-C₆₀ form was first measured at 1000 nm (left side of Figure 6). Laser excitation (650 nm) generates BT^{•-}-P⁺-C₆₀ via photoinduced electron transfer from the porphyrin to the betaine, and this state rapidly recombines, leaving only residual absorbance that comes mainly from the fullerene radical anion generated in the portion of the sample that is still in the DHI-P-C₆₀ form. The sample was then irradiated for 40 min with visible (≥ 590 nm) light from a xenon lamp, which also caused some local heating. The combined effects of the light and heating caused virtually complete isomerization of BT-P-C₆₀ to the DHI-P-C₆₀ form **1c**. Laser excitation of **1c** led to photoinduced electron transfer from the porphyrin to the fullerene, giving DHI-P⁺-C₆₀^{•-}. Subsequently, the sample was irradiated for 1.5 min with 366 nm light, driving isomerization of DHI-P-C₆₀ back to the original BT-P-C₆₀ form **1o**. Charge separation then switches back to the other arm of the molecule. The cycles were repeated 7 times, demonstrating reasonable photochemical stability for the system.

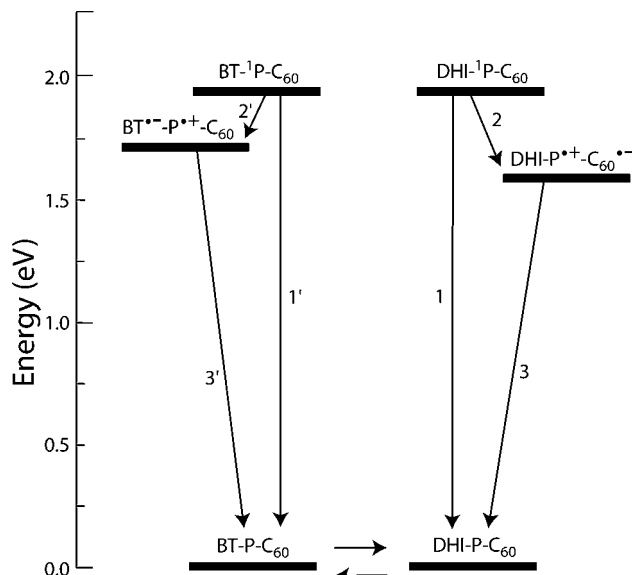


Figure 7. Transient states and relevant interconversion pathways for triad **1** with the photochromic moiety in the open, **1o**, form (left) and the closed, **1c**, form (right).

Discussion

Energetics. To interpret the photochemical results, we need estimates of the energies of the various excited states and charge-separated states. The energy of the porphyrin first excited singlet state, estimated from the wavenumber average of the longest wavelength absorption maximum and the shortest-wavelength emission band, is 1.91 eV above the ground state. Redox potentials of model compounds measured by cyclic voltammetry were used to estimate the energies of the charge-separated states. The first oxidation potential of model porphyrin **3** is 1.03 V versus SCE, measured in benzonitrile with 0.1 M tetra-*n*-butylammonium hexafluorophosphate as supporting electrolyte and ferrocene as an internal standard.¹⁶ The first reduction potential of a model for the fullerene in **1**, measured under the same conditions, is -0.56 V.¹⁷ The first reduction potentials for the DHI moiety are -1.18 V for the DHI form and -0.70 V for the betaine form.⁹ Thus, the DHI-P⁺-C₆₀^{•-} state is estimated to be 1.59 eV above the molecular ground state, and the BT^{•-}-P⁺-C₆₀ state 1.73 eV above the ground state. On the basis of these data, a diagram showing the energetics of the various relevant states of **1** and some of their potential interconversion pathways has been constructed (Figure 7).

Electron-Transfer Kinetics. The spectroscopic results for P-C₆₀ dyad **9** and DHI-P dyad **2** will be discussed, and the information obtained will then be used to decipher the data for triad **1**. The quenching of the porphyrin fluorescence in P-C₆₀ dyad **9** is ascribed to photoinduced electron transfer to form the P⁺-C₆₀^{•-} charge-separated state. The formation of this state is verified by the transient absorption results, showing the fullerene radical anion absorption at ~ 1010 nm and absorption of the porphyrin radical cation in the visible region of the spectrum. Although singlet energy transfer from ¹P-C₆₀ to the fullerene to yield P-¹C₆₀ at 1.75 eV is also energetically

- (16) Gould, S. L.; Kodis, G.; Palacios, R. E.; de la Garza, L.; Brune, A.; Gust, D.; Moore, T. A.; Moore, A. L. *J. Phys. Chem. B* **2004**, *108*, 10566–10580.
 (17) Kodis, G.; Liddell, P. A.; de la Garza, L.; Moore, A. L.; Moore, T. A.; Gust, D. *J. Mater. Chem.* **2002**, *12*, 2100–2108.

possible and may occur to some extent, no evidence for this process was observed in 2-methyltetrahydrofuran. In the absence of energy transfer, the rate constant for photoinduced electron transfer, k_{ET} , is given by eq 1

$$k_{\text{ET}} = (1/\tau_s) - k_D \quad (1)$$

where τ_s is the lifetime of the porphyrin excited singlet state of **9** (2.0 ns), and k_D is the rate constant for decay of the excited state in the absence of electron transfer. We estimate k_D as $9.9 \times 10^7 \text{ s}^{-1}$ from the 10.1 ns lifetime of the first excited singlet state of model porphyrin **3**. Thus, $k_{\text{ET}} = 4.0 \times 10^8 \text{ s}^{-1}$. The quantum yield of photoinduced electron transfer is $k_{\text{ET}} \times \tau_s$, or 80%. The $\text{P}^{+\bullet}-\text{C}_{60}^{\bullet-}$ state decays with a rate constant k_{CR} of $\sim 2.5 \times 10^8 \text{ s}^{-1}$, as determined from the 4 ns lifetime measured by transient absorption spectroscopy.

The corresponding rate constants for model dyad **2** have been reported.⁹ In the DHI-P form of the dyad, the porphyrin first excited singlet state is unquenched, and electron transfer does not occur. In the BT-P form, electron transfer occurs from BT-¹P to yield $\text{BT}^{\bullet-}-\text{P}^{+\bullet}$ with a rate constant k'_{ET} of $2.0 \times 10^{10} \text{ s}^{-1}$ and a quantum yield of 1.0. Recombination of $\text{BT}^{\bullet-}-\text{P}^{+\bullet}$ to the ground state occurs rapidly, with $k'_{\text{CR}} = 3.4 \times 10^{11} \text{ s}^{-1}$.

Turning now to triad **1**, we find that the photochemical behavior is basically a superposition of the processes in model compounds **2** and **9**. In the closed form of the triad, DHI-P-C₆₀, the porphyrin first excited singlet state decays with a time constant of 1.9 ns (from the time-resolved fluorescence results) to yield the $\text{DHI}-\text{P}^{+\bullet}-\text{C}_{60}^{\bullet-}$ charge-separated state. The rate constant for photoinduced electron transfer (k_2 , for step 2 in Figure 7) may be calculated using an equation similar to eq 1 and taking k_1 (step 1 in Figure 7) as $9.9 \times 10^7 \text{ s}^{-1}$, based on the results for model porphyrin **3**. The value obtained is $4.3 \times 10^8 \text{ s}^{-1}$, and the quantum yield of $\text{DHI}-\text{P}^{+\bullet}-\text{C}_{60}^{\bullet-}$ is 82%. From the 4.7 ns lifetime of this charge-separated state measured using transient absorption spectroscopy (Figure 5), k_3 equals $2.1 \times 10^8 \text{ s}^{-1}$. Although Figure 7 depicts recombination of $\text{DHI}-\text{P}^{+\bullet}-\text{C}_{60}^{\bullet-}$ directly to the ground state, some recombination to give a triplet state cannot be excluded.

Excitation of the porphyrin moiety of the open, BT-P-C₆₀ isomer **1o** is also followed by photoinduced electron transfer, but in this case the product is $\text{BT}^{\bullet-}-\text{P}^{+\bullet}-\text{C}_{60}$. The rate constant for this process, k_2' , may be calculated using eq 2

$$1/\tau_{s'} = k_1' + k_2' + k_2 \quad (2)$$

where $\tau_{s'}$ is the lifetime of the porphyrin first excited singlet state of **1o** (taken as 55 ps from the transient absorption data), k_1' is the rate constant for decay of this state by the usual photophysical processes in the absence of electron transfer (taken as $9.9 \times 10^7 \text{ s}^{-1}$ from the results for model porphyrin **3**), and k_2 is the rate constant for photoinduced electron transfer to the fullerene moiety (taken as $4.3 \times 10^8 \text{ s}^{-1}$ from the results for **1c**). A value for k_2' of $1.8 \times 10^{10} \text{ s}^{-1}$ is calculated. This corresponds to a quantum yield of 99% for $\text{BT}^{\bullet-}-\text{P}^{+\bullet}-\text{C}_{60}$. The yield of $\text{BT}-\text{P}^{+\bullet}-\text{C}_{60}^{\bullet-}$ via electron transfer down the wrong path is only $\sim 1\%$. Of course, in an actual solution of the molecules, a fraction is in the DHI-P-C₆₀ form at the photostationary state when 366 nm irradiation is employed. No

attempt was made to find the optimum wavelength for maximizing the population of the betaine form.

From these results, it is clear that triad **1** performs as a molecular double-throw switch. This is easily seen from Figure 6. On the left side of Figure 6, the transient absorbance at 1000 nm 5 ns after 650 nm excitation was measured for the molecule in the open, BT-P-C₆₀ form **1o**. In this form, 99% of the photons absorbed by the porphyrin result in formation of $\text{BT}^{\bullet-}-\text{P}^{+\bullet}-\text{C}_{60}$; photoinduced electron transfer occurs from the porphyrin to the betaine moiety. The residual absorbance at 1000 nm is due to $\text{C}_{60}^{\bullet-}$ from the **1c** still present and possibly some decomposition due to irradiation. Irradiation of the sample with light $\geq 590 \text{ nm}$ for 40 min photoisomerizes the molecule to the DHI-P-C₆₀ form **1c**. Excitation of the sample with 650 nm laser pulses then generates the $\text{DHI}-\text{P}^{+\bullet}-\text{C}_{60}^{\bullet-}$ charge-separated state via photoinduced electron transfer from the porphyrin to the fullerene. The switch has been thrown, and electrons flow down the second pathway. Irradiation with 366 nm light for 1.5 min switches the molecule back to the BT-P-C₆₀ form, and the transient absorbance at 1000 nm again drops. It is clear from Figure 6 that little or no photodecomposition has occurred during the cycles shown. The variations in absolute amplitude of the transient absorbance when the molecule is in either the **1o** or **1c** form are due to variations in light flux from the excitation laser.

Conclusions

Molecule **1** has been shown to function as a double-throw switch for photoinduced electron transfer, with switching between production of two charge-separated states due to photoisomerization of the dihydroindolizine moiety. The quantum yield of one charge-separated state is 99% when the molecule is in the open, BT-P-C₆₀ form, while the yield of the second charge-separated state is 82% when the triad is in the DHI-P-C₆₀ state. Thus, the excited porphyrin moiety sends an electron down one arm of the molecule or the other, based on the state of the photochromic switch. In either form of the molecule, 1% or less of the porphyrin excited states decay by electron transfer along the wrong pathway. The molecule is relatively stable toward photodecomposition under the conditions employed here. This result, coupled with other examples of photochemically operated switches and logic gates, may help point the way to photonic control of electron flow at the molecular level, with possible applications to data processing, storage, and transmission; biomimetic signaling; and solar energy conversion.

Experimental Procedures

Instrumental Techniques. The ¹H NMR spectra were recorded on Varian Unity spectrometers at 300 or 500 MHz. Samples were dissolved in deuteriochloroform with tetramethylsilane as an internal reference. Mass spectra were obtained on a matrix-assisted laser desorption/ionization time-of-flight spectrometer (MALDI-TOF). The solvent for all spectroscopic measurements was freshly distilled 2-methyltetrahydrofuran, unless otherwise stated. All samples were deoxygenated by bubbling with argon for 20 min. Ground-state absorption spectra were measured on a Shimadzu UV-3101PC UV-vis-NIR spectrometer. Steady-state fluorescence emission spectra were measured using a Photon Technology International MP-1 fluorometer and corrected. Excitation was produced by a 75 W xenon lamp and single grating monochromator. Fluorescence was detected at 90° to the excitation beam via a single grating monochromator and an R928 photomultiplier

tube having S-20 spectral response operating in the single-photon-counting mode.

Fluorescence decay measurements were performed on $\sim 1 \times 10^{-5}$ M solutions by the time-correlated single-photon-counting method. The excitation source was a cavity-dumped Coherent 700 dye laser pumped by a frequency-doubled Coherent Antares 76s Nd:YAG laser. Fluorescence emission was detected at a magic angle using a single grating monochromator and microchannel plate photomultiplier (Hamamatsu R2809U-11). The instrument response time was ca. 35–50 ps, as verified by scattering from Ludox AS-40 at the excitation wavelength.¹⁸

Nanosecond transient absorption measurements were made with excitation from an OPOTEK optical parametric oscillator driven by the third harmonic of a Continuum Surelight Nd:YAG laser (650 nm). The pulse width was ~ 5 ns, and the repetition rate was 10 Hz. The detection portion of the spectrometer was manufactured by Ultrafast Systems.

The femtosecond transient absorption apparatus consisted of a kHz pulsed laser source and a pump–probe optical setup. The laser pulse train was provided by a Ti:Sapphire regenerative amplifier (Clark-MXR, Model CPA-1000) pumped by a diode-pumped CW solid-state laser (Spectra Physics, Model Millennia V). The typical laser pulse was 100 fs at 790 nm, with a pulse energy of 0.9 mJ at a repetition rate of 1 kHz. Most of the laser energy (80%) was used to pump an optical parametric amplifier (IR-OPA, Clark-MXR). The excitation pulse was sent through a computer-controlled optical delay line. The remaining laser output (20%) was focused into a 1.2 cm rotating quartz plate to generate a white light continuum. The continuum beam was further split into two identical parts and used as the probe and reference beams, respectively. The probe and reference signals were focused onto two separated optical fiber bundles coupled to a spectrograph (Acton Research, Model SP275). The spectra were acquired on a dual diode array detector (Princeton Instruments, Model DPDA-1024).¹⁹ To determine the number of significant components in the transient absorption data, singular value decomposition analysis^{20,21} was carried out using locally written software based on the MatLab 5.0 program (MathWorks, Inc.).

The photoinduced opening and closing kinetics of the triad were studied using, respectively, a UVP UV lamp Model UVGL-25 and a Xe/HgXe-lamp (ORIEL Corp. Model 66028). Before sample illumination with the Xe lamp, the IR portion of the light was reduced by the beam being passed through two water-cooled IR filters ($A = 1.8$ and 2.3 at 900 and 970 nm, respectively). Furthermore, a long-pass filter was used to remove wavelengths shorter than 590 nm.

Synthesis. Using previously reported methods,^{15,16} 4,4'-[10,20-bis-(2,4,6-trimethylphenyl)-21*H*,23*H*-porphine-5,15-diyl]bis[benzoic acid] dimethyl ester **3** was prepared and converted to 4-[15-(4-aminophenyl)-10,20-bis(2,4,6-trimethylphenyl)-21*H*-23*H*-porphine-5-yl]benzoic acid **4**.

4-[15-(4-Aminophenyl)-10,20-bis(2,4,6-trimethylphenyl)-21*H*-23*H*-porphine-5-yl]benzoic Acid *t*-Butyl Ester (5**).** Porphyrin **4** (220 mg, 0.290 mmol) was dissolved in 9 mL of anhydrous *N,N*-dimethylacetamide containing 128 mg (0.562 mmol) of benzyltriethylammonium chloride and 1.8 g (13 mmol) of dry K_2CO_3 . The reaction mixture was heated to 55 °C under N_2 before 2.64 mL (23 mmol) of 2-bromo-2-methylpropane was added. After 17 h, the reaction was cooled, diluted with dichloromethane, and washed repeatedly with water. The organic layer was distilled at reduced pressure, and the residue was chromatographed (silica gel, 8:92 MeOH:CH₂Cl₂) to give 173 mg (0.213 mmol) of **5** (73%): ¹H NMR (300 MHz, CDCl₃) δ -2.60 (2H, s, N-H), 1.76 (9H, s, *t*-Bu-H), 1.83 (12H, s, Ar-CH₃), 2.63 (6H, s, Ar-CH₃), 4.04 (2H, brs, -NH₂), 7.06 (2H, d, $J = 8.7$ Hz,

Ar-H), 7.28 (4H, s, Ar-H), 8.00 (2H, d, $J = 8.7$ Hz, Ar-H), 8.27 (2H, d, $J = 8.1$ Hz, Ar-H), 8.36 (2H, d, $J = 8.1$ Hz, Ar-H), 8.68–8.90 (8H, m, β -pyrrole H); MALDI-TOF calcd for C₅₅H₅₁N₅O₂ 813.40; obsd 813.37; UV/vis (dichloromethane) 421, 517, 555, 595, 649 nm.

4-[15-(4-[(Pyridazine-4-carbonyl)-aminol]-phenyl)-10,20-bis-(2,4,6-trimethylphenyl)-21*H*,23*H*-porphine-5-yl]benzoic acid *t*-butyl ester (6**)** was prepared by dissolving 170 mg (0.208 mmol) of **5** in 15 mL of dichloromethane along with 56 mg (0.45 mmol) of pyridazine 4-carboxylate and 27 mg (0.22 mmol) of 4-(dimethylamino)pyridine. After the mixture was cooled to 0 °C, 84 mg (0.44 mmol) of 1-[3-(dimethylamino)propyl]-3-ethylcarbodiimide hydrochloride was added; after 10 min, the ice bath was removed. The reaction mixture was stirred for 22 h, diluted with dichloromethane, and washed with water, and the solvent was evaporated at reduced pressure. Chromatography (silica gel, 30:70 acetone/dichloromethane) yielded 150 mg (0.163 mmol) of **6** (78%): ¹H NMR (300 MHz, CDCl₃) δ -2.62 (2H, s, N-H), 1.76 (9H, s, *t*-Bu-H), 1.84 (12H, s, -CH₃), 2.62 (6H, s, -CH₃), 7.28 (4H, s, Ar-H), 8.08–8.12 (4H, m, Ar-H), 8.28 (2H, d, $J = 8.7$, Ar-H), 8.70–8.84 (8H, m, β -pyrrole H), 9.52–9.54 (1H, m, pyridazine-H), 9.81 (1H, brs, pyridazine-H); MALDI-TOF m/z calcd for C₆₀H₅₃N₇O₃ 919.42; obsd 919.41; UV/vis (dichloromethane) 419, 515, 550, 590, 646 nm.

Benzyl *N*-(4-Cyanophenyl)carbamate (10**).** A 1 g (8.47 mmol) portion of *p*-cyanoaniline was suspended in 10 mL of 1 M NaOH, 3 mL THF was added, and the mixture was cooled to 0 °C. Benzylchloroformate (1.8 mL, 12.6 mmol) was slowly added, followed by 5 mL of 2 M aqueous NaOH. After 10 min, the yellow solution turned white; 10 mL of acetone and 5 mL of 2 M NaOH were added. After being stirred overnight, the reaction mixture was diluted with ethyl acetate, and the organic layer was washed with citric acid and water and dried over MgSO₄. The solvent was evaporated under reduced pressure. The residue was chromatographed (silica gel, 10:90 ethyl acetate/toluene), and 954 mg (3.78 mmol) of **10** was isolated (45%): ¹H NMR (300 MHz, CDCl₃) δ 5.22 (2H, s, -CH₂-), 6.86 (1H, s, N-H), 7.37–7.41 (5H, m, Ar-H), 7.51 (2H, d, $J = 9$ Hz, Ar-H), 7.59 (2H, d, $J = 9$ Hz, Ar-H).

Benzyl *N*-(4-Formylphenyl)carbamate (11**).** This previously reported²² compound was prepared as follows. In 25 mL of tetrahydrofuran was dissolved 0.750 g (2.98 mmol) of **10**, and the mixture was cooled to -40 °C. Diisobutylaluminum hydride in heptane (15 mL of a 1.0 M solution, 15 mmol) was added slowly by addition funnel under N_2 . The reaction mixture was allowed to warm gradually to room temperature and was stirred overnight. Hydrochloric acid (10 mL of a 2 M solution) was added, and the mixture was stirred for 10 min before being washed with water and aqueous NaHCO₃. The organic layer was diluted with toluene and dried with MgSO₄, and the solvent was evaporated at reduced pressure. The residue was chromatographed (silica gel, 40:60 ethyl acetate/hexanes), and 165 mg (0.65 mmol) of **11** was isolated (22%): ¹H NMR (300 MHz, CDCl₃) δ 5.21 (2H, s, -CH₂-), 7.08 (1H, s, N-H), 7.35–7.41 (5H, m, Ar-H), 7.56 (2H, d, $J = 8$ Hz, Ar-H), 7.82 (2H, d, $J = 8$ Hz, Ar-H), 9.89 (1H, s, -CHO).

Benzyl *N*-(4-(1',5'-Dihydro-1'-methyl-2'*H*-[5,6]fullereno-C₆₀-I_h-[1,9-*c*]pyrrole-2'-yl)phenyl)carbamate (7**).** Aldehyde **11** (50 mg, 196 mmol) was added to 75 mL of toluene as were 282 mg (392 mmol) of C₆₀ and 174 mg (1.96 mmol) of sarcosine. The reaction mixture was heated to reflux under N_2 for 20 h, after which the solvent was evaporated at reduced pressure. The residue was redissolved in dichloromethane and filtered, and the solvent was again evaporated. The residue was chromatographed (silica gel, 3:97 ethyl acetate/toluene) to give 76 mg (0.076 mmol) of **7** (39%): ¹H NMR (300 MHz, CDCl₃) δ 2.79 (3H, s, N-CH₃), 4.24 (1H, d, $J = 9.3$, -N-CH₂-)

- (18) Gust, D.; Moore, T. A.; Luttrull, D. K.; Seely, G. R.; Bittersmann, E.; Bensasson, R. V.; Rougée, M.; Land, E. J.; de Schryver, F. C.; Van der Auweraer, M. *Photochem. Photobiol.* **1990**, *51*, 419–426.
(19) Freiberg, A.; Timpmann, K.; Lin, S.; Woodbury, N. W. *J. Phys. Chem. B* **1998**, *102*, 10974–10982.

- (20) Golub, G. H.; Reinsch, C. *Numer. Math.* **1970**, *14*, 403–420.
(21) Henry, E. R.; Hofrichter, J. In *Methods in Enzymology*; Ludwig, B., Ed.; Academic Press: San Diego, 1992; p 219.
(22) Witke, S.; Bielawski, J.; Bielawska, A. *J. Prakt. Chem./Chem.-Ztg.* **1979**, *321*, 804–812.

4.89 (1H, s, $-N-CH-$), 4.97 (1H, d, $J = 9.3$, $-N-CH_2-$), 5.19 (2H, s, $-CH_2-$), 6.70 (1H, s, $-N-H$), 7.31–7.40 (5H, m, Ar-H), 7.46 (2H, d, $J = 9$ Hz, Ar-H), 7.73 (2H, brm, Ar-H); MALDI-TOF m/z calcd for $C_{77}H_{18}N_2O_2$ 1002.11; obsd 1002.14; UV/vis (dichloromethane) 702 nm.

DHI-P dyad (8). In 18 mL of freshly distilled tetrahydrofuran in a 50 mL round-bottom flask fitted with a septum was dissolved 58 mg (0.063 mmol) of **6**. The solution was degassed by three freeze–pump–thaw cycles. After the flask was backfilled with argon, 118 mg (0.441 mmol) of spiro[fluorene-9,3'-[3H]pyrazole]-4',5'-dicarbonitrile^{23,24} was added as a solid, and the mixture was irradiated for 45 min with a 450 W medium-pressure mercury lamp through a Pyrex 7740 filter. After this time, thin-layer chromatography indicated that the reaction was not yet complete. Another 50 mg (0.19 mmol) of spiro[fluorene-9,3'-[3H]pyrazole]-4',5'-dicarbonitrile was added, and the solution was irradiated for another 30 min. Following irradiation, the reaction was kept in the dark overnight to allow thermal conversion of the product to the closed form. Column chromatography (silica gel, dichloromethane) followed by a second column (silica gel, 40:60 ethyl acetate/hexanes) was performed to purify the product and separate it from its isomer to yield 30 mg (0.026 mmol, 44%) of **8**: 1H NMR (300 MHz, $CDCl_3$) δ –2.64 (2H, s, N-H), 1.75 (9H, s, t -Bu-H), 1.81 (12H, s, Ar-CH₃), 2.62 (6H, s, Ar-CH₃), 5.52 (1H, d, $J = 2.4$ Hz, pyridazine CH), 5.77 (1H, dd, $J = 2.4$ Hz, 2.1 Hz, pyridazine C=CH–), 7.27 (4H, s, Ar-H) 7.41–7.87 (9H, m, fluorene Ar-H, amide N-H), 7.69 (1H, d, $J = 2.1$ Hz, pyridazine N=CH–), 7.73 (2H, d, $J = 8.7$ Hz, Ar-H), 8.12 (2H, d, $J = 8.7$ Hz, Ar-H), 8.26 (2H, d, $J = 8.1$ Hz, Ar-H), 8.36 (2H, d, $J = 8.1$ Hz, Ar-H), 8.65–8.75 (8H, m, β -pyrrole H); MALDI-TOF m/z calcd for $C_{77}H_{61}N_9O_3$ 1159.49; obsd 1159.47.

P-C₆₀ Dyad (9). Fullerene precursor **7** (11.5 mg, 0.011 mmol) was dissolved in 50 mL of dichloromethane and cooled to -78 °C under a nitrogen atmosphere before 0.4 mL of 1.0 M BBr_3 solution in dichloromethane was added. After being stirred for 30 min, the reaction was warmed to room temperature and stirred for 1 h, whereupon 25 mL of pyridine was added. The dichloromethane was evaporated at reduced pressure, and 1.0 mg (0.0082 mmol) of 4-(dimethylamino)pyridine and 20 mg (0.025 mmol) of 4,4'-[10,20-bis(2,4,6-trimethylphenyl)-21H,23H-porphine-5,15-diyl]bis[benzoic acid] monomethyl ester¹⁵ were added to the remaining pyridine solution. This solution was cooled to 0 °C before 3 mg (0.016 mmol) of 1-[3-(dimethylamino)propyl]-3-ethylcarbodiimide hydrochloride was added. After 5 min, the ice bath was removed, and the reaction mixture was stirred in the dark for 20 h. The solvent was evaporated under reduced pressure, and the residue was chromatographed (silica gel, 5:95 ethyl acetate/toluene) to give 12 mg of **9** (63%): 1H NMR (300 MHz, $CDCl_3$) δ –2.63 (2H, s, N-H), 1.83 (12H, s, $-CH_3$), 2.62 (6H, s, $-CH_3$), 2.86 (3H, s, N-CH₃), 4.10 (3H, s, COOCH₃), 4.29 (1H, d, $J = 9.3$, pyrrolid-

CH₂–), 4.96 (1H, s, pyrrolid-CH–), 4.99 (1H, d, $J = 9.3$, pyrrolid-CH₂–), 7.25 (4H, s, Ar-H), 7.89 (4H, brs, Ar-H), 8.18–8.23 (3H, m, Ar-H, amide-H), 8.27–8.33 (4H, m, Ar-H), 8.41 (2H, d, $J = 8.4$ Hz, Ar-H), 8.68–8.73 (8H, m, β -pyrrole H); MALDI-TOF m/z calcd for $C_{122}H_{54}N_6O_3$ 1651.43; obsd 1651.41.

Triad 1. Dyad **8** (35 mg, 0.030 mmol) was dissolved in 4 mL of dichloromethane; 10 μ L of triethylsilane and 1.8 mL of trifluoroacetic acid were added, and the reaction mixture was stirred in the dark. After 4.5 h, the reaction mixture was diluted with dichloromethane and washed with water until neutral, the solvent was evaporated at reduced pressure, and the residue was redissolved in 7 mL of dichloromethane. Thin-layer chromatography indicated that the t -butyl ester had been >95% cleaved to give the free acid. Meanwhile, 36 mg (0.036 mmol) of **7** was dissolved in 40 mL of dichloromethane and cooled to -78 °C under N_2 , and 1 mL of 1 M BBr_3 in heptane was added. This reaction mixture was stirred under N_2 for 30 min before being warmed to room temperature. After being stirred for an additional 1.5 h, the reaction mixture was washed with water, 5% aqueous $NaHCO_3$, and then repeatedly with water. Pyridine was added periodically throughout the washings to keep **7** in its deprotected, amino form soluble. The resulting solution was concentrated to a volume of 10 mL by evaporation of the solvent at reduced pressure and then combined with the carboxylic acid form of dyad **8**, prepared as described previously, and dissolved in 7 mL of dichloromethane. To the resulting solution was added 10 mg (0.048 mmol) of 1,3-dicyclohexylcarbodiimide, and the reaction mixture was stirred under N_2 for 40 h. The reaction mixture was then washed twice with 0.25 M citric acid in water and repeatedly with water, the organic layer was concentrated by evaporation of the solvent at reduced pressure, and the residue was chromatographed (silica gel, 5:95 ethyl acetate/toluene followed by silica gel 1:99 acetone/dichloromethane) to give 4.5 mg (0.0023 mmol) of **1** (8.2%): 1H NMR (500 MHz $CDCl_3$) δ –2.66 (2H, s, NH), 1.81 (12H, s, Me-CH₃), 2.62 (6H, s, Me-CH₃), 2.86 (3H, s, N-CH₃), 4.29 (1H, d, $J = 9$ Hz, pyrrolid-CH₂), 4.98 (1H, s, pyrrolid-CH), 5.01 (1H, d, $J = 9$ Hz, pyrrolid-CH₂), 5.52 (1H, d, $J = 2.5$ Hz, pyridazine CH), 5.76 (1H, dd, $J = 2.5$ Hz, $J = 2.5$ Hz, pyridazine C=CH–), 7.27 (4H, s, Ar-H), 7.43–7.68 (7H, m, fluorene Ar-H, amide N-H), 7.70 (1H, d, $J = 2.5$ Hz, pyridazine N=CH–), 7.75 (2H, d, $J = 8.5$ Hz, Ar-H), 7.82–7.87 (2H, m, fluorene Ar-H), 7.89 (4H, brm, pyrrolid-phenyl-H), 8.14 (2H, d, $J = 8.5$ Hz, Ar-H), 8.19 (1H, s, C₆₀-P_{2H} amide N-H), 8.22 (2H, d, $J = 8$ Hz, Ar-H), 8.32 (2H, d, $J = 8$ Hz, Ar-H), 8.66–8.73 (8H, m, β -pyrrole H); MALDI-TOF calcd for $C_{142}H_{63}N_{11}O_2$ 1954.52; obsd 1954.43.

Acknowledgment. This work was supported by a grant from the National Science Foundation (CHE-0352599). This is publication No. 600 from the ASU Center for the Study of Early Events in Photosynthesis. J.A. thanks the Carl Trygger Foundation for Scientific Research for postdoctoral support.

JA044128I

(23) Dürr, H. Photochromism of dihydroindolizines and related systems; In *Organic Photochromic and Thermochromic Compounds*; Crano, J. C., Guglielmetti, R. J., Eds.; Plenum Press: New York, 1999; pp 223–266.

(24) Gross, H.; Dürr, H. *Angew. Chem., Int. Ed. Engl.* **1982**, *21*, 216–217.